

Electron Energy Loss Spectroscopy of LiMn_2O_4 , and $\text{LiMn}_{1.5}\text{Ni}_{0.5}\text{O}_4$

S.M. Loya-Mancilla, L. Alvarez-Contreras, D. Carrillo-Flores, M.T. Ochoa-Lara, A. Aguilar-Elguezabal, F. Espinosa-Magaña

Centro de Investigación en Materiales Avanzados, Laboratorio Nacional de Nanotecnología, Miguel de Cervantes No.120, C.P. 31109, Chihuahua, Chihuahua, México.

The use of rechargeable batteries has become a standard for mobile applications being, for many years, LiCoO_2 the most common material used for the cathode. However, the toxicity of cobalt and its high cost has stimulated the search of alternative materials to substitute cobalt by a cheaper and environmental friendly material. One of the most promissory materials to fulfill these requirements is the spinel LiMn_2O_4 . Recently, several new spinel manganates, where the Mn 16d site of the spinel structure is partially substituted by a third cation, have been studied extensively. These materials overcome the disadvantages of stoichiometric spinel LiMn_2O_4 and still posses a spinel structure.

In this work, the dielectric properties of LiMn_2O_4 and $\text{LiMn}_{1.5}\text{Ni}_{0.5}\text{O}_4$ powders, synthesized by sol-gel method, were determined by analyzing the low loss region of the EELS spectrum in a transmission electron microscope. These spectra can be interpreted on the basis of *ab initio* calculations. Theoretical calculations are based on the pseudo-potential plane-wave method within the framework of the density functional theory (DFT), as implemented in CASTEP code. Norm-conserving pseudopotentials were employed to describe the electron-ion interactions. The exchange and correlation terms were described with the generalized gradient approximation (GGA). An energy cutoff $E_{\text{cut}} = 550$ eV was chosen, and self-consistency was considered to be achieved when the total energy variation from iteration to iteration did not exceed 5×10^{-7} eV/atom. For the substituted spinel $\text{LiMn}_{1.5}\text{Ni}_{0.5}\text{O}_4$ a $2 \times 1 \times 1$ supercell was constructed. The crystal structures of the lithium manganate spinel and substituted spinel were taken from experimental results.

Electron energy loss spectra were obtained using a Gatan Parallel Electron Energy Loss Spectrometer (PEELS model 766) attached to a Philips CM-200 transmission electron microscope. Spectra were acquired in diffraction mode with 0.2 eV/ch dispersion, an aperture of 2 mm and a collection semi-angle of about 2.7 mrad. The resolution of the spectra was determined by measuring the full width at half-maximum (FWHM) of the zero loss peak and this was typically close to 1.2 eV, when the TEM was operated at 200 kV. EELS spectra were corrected for dark current and readout noise. The channel to channel gain variation was minimized by normalizing the experimental spectrum with independently obtained gain spectrum of the spectrometer.

Figs. 1 and 2 show the energy loss function and the Kramers-Kronig derived imaginary part of the dielectric function, respectively, for LiMn_2O_4 (black) and $\text{LiMn}_{1.5}\text{Ni}_{0.5}\text{O}_4$. Figs. 3-6 show results from theoretical calculations with the CASTEP code. Figs. 3 and 5 show the energy loss function. Figs. 4 and 6 show the imaginary part of the dielectric function of LiMn_2O_4 and $\text{LiMn}_{1.5}\text{Ni}_{0.5}\text{O}_4$, respectively. From the calculated real part of the dielectric function (not shown), we can identify well defined plasmon peaks at 8.9 and 22.4 eV for LiMn_2O_4 and at 9.0 and 24.4 eV for $\text{LiMn}_{1.5}\text{Ni}_{0.5}\text{O}_4$. Experimental (EELS) results show plasmon peaks at 10.2 and 22.8 eV for the spinel and 9.0 and 24.4 eV for the substituted spinel, which agree relatively well with the calculated values. The other peaks come from interband transitions and reflect the energy band structure of the materials.

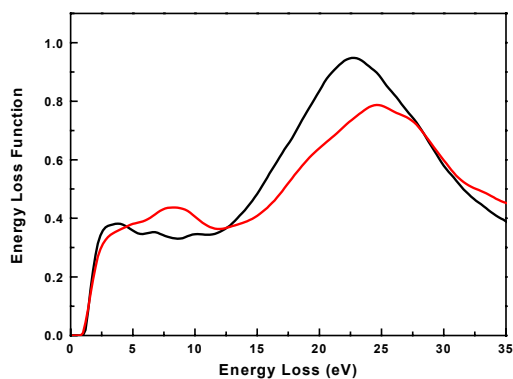


Fig. 1. Energy Loss Function of LiMn_2O_4 (black) and $\text{LiMn}_{1.5}\text{Ni}_{0.5}\text{O}_4$ (red)

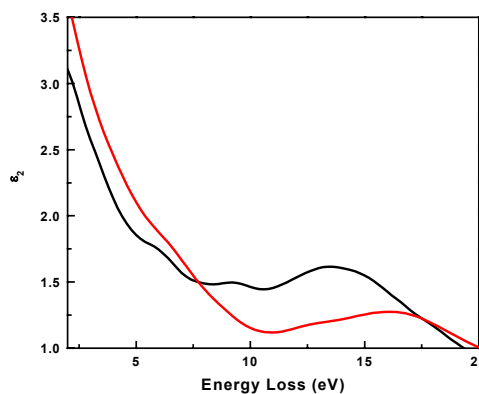


Fig. 2. Imaginary part of the dielectric function of LiMn_2O_4 (black) and $\text{LiMn}_{1.5}\text{Ni}_{0.5}\text{O}_4$ (red)

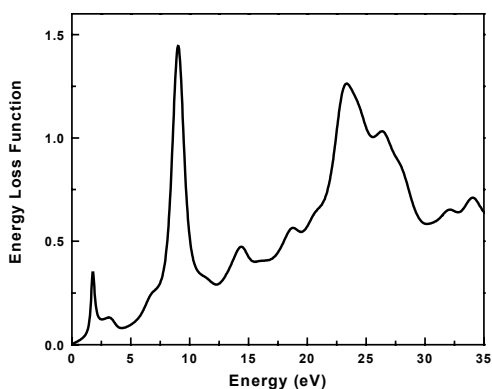


Fig. 3. Calculated energy loss function of LiMn_2O_4

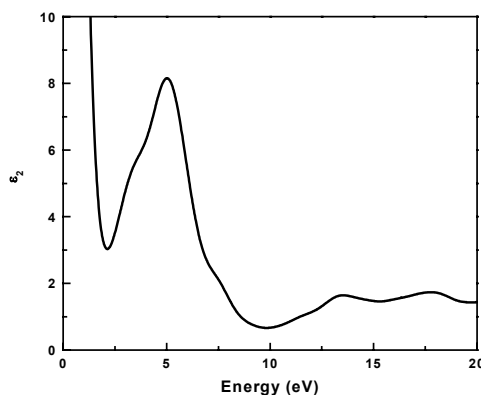


Fig. 4. Calculated imaginary part of the dielectric function of LiMn_2O_4

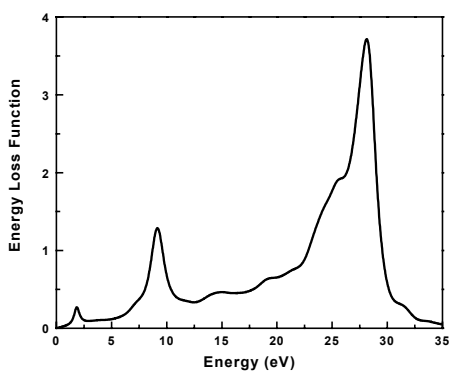


Fig. 5. Calculated energy loss function of $\text{LiMn}_{1.5}\text{Ni}_{0.5}\text{O}_4$

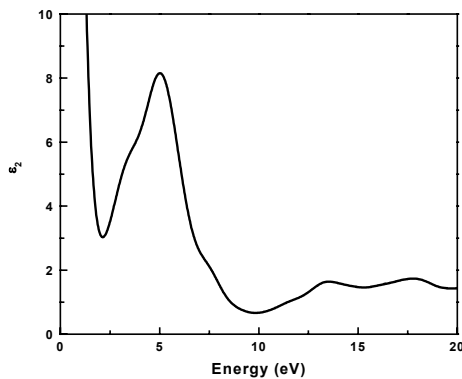


Fig. 6. Calculated imaginary part of the dielectric function of $\text{LiMn}_{1.5}\text{Ni}_{0.5}\text{O}_4$